BIOLOGY OF REPRODUCTION (2012) **86**(5):150, 1–8
Published online before print 22 February 2012.
DOI 10.1095/biolreprod.111.095158

Peritubular Myoid Cells from Rat Seminiferous Tubules Contain Actin and Myosin Filaments Distributed in Two Independent Layers[1]

Antonella D. Losinno, Alfonsina Morales, Dario Fernández, and Luis A. Lopez[2]

Laboratory of Cytoskeleton and Cell Cycle, Instituto de Histología y Embriología, Facultad de Ciencias Médicas, Universidad Nacional de Cuyo, Mendoza, Argentina

ABSTRACT

In the mammalian testis, peritubular myoid cells (PM cells) surround the seminiferous tubules (STs), express cytoskeletal markers of true smooth muscle cells, and participate in the contraction of the ST. It has been claimed that PM cells contain bundles of actin filaments distributed orthogonally in an intermingled mesh. Our hypothesis is that these actin filaments are not forming a random intermingled mesh, but are actually arranged in contractile filaments in independent layers. The aim of this study is to describe the organization of the actin cytoskeleton in PM cells from adult rat testes and its changes during endothelin-1-induced ST contraction. For this purpose, we isolated segments of ST corresponding to the stages IX–X of the spermatogenic cycle (ST segments), and analyzed the actin and myosin filament distribution by confocal and transmission electron microscopy. We found that PM cells have actin and myosin filaments interconnected in thick bundles (AF-MyF bundles). These AF-MyF bundles are distributed in two independent layers: an inner layer toward the seminiferous epithelium, and an outer layer toward the interstitium, with the bundles oriented perpendicularly and in parallel to the main ST axis, respectively. In endothelin-1 contracted ST segments, PM cells increased their thickness and reduced their length in both directions, parallel and perpendicular to the main ST axis. The AF-MyF bundles maintained the same organization in two layers, although both layers appeared significantly thicker. We believe that this is the first time this arrangement of AF-MyF bundles in two independent layers has been shown in smooth muscle cells, and that this organization would allow the cell to generate contractile force in two directions.

actin filament, contraction, myosin filament, peritubular myoid cell, seminiferous tubule

INTRODUCTION

In rodent testis, peritubular myoid (PM) cells) have a flat polygonal shape and form a monolayer surrounding the seminiferous tubules (STs) [1, 2]. The PM cells are in contact with two basement membranes (BMs). One BM is oriented toward the germinal epithelium, and the other is oriented toward the endothelial cells and the interstitium [3].

Peritubular myoid cells evince contractile function and express cytoskeletal markers of smooth muscle, such as alpha-isoactin and smooth muscle myosin. The contractile activity of PM cells is involved in the transport of spermatozoa and testicular fluid through the ST [4].

It has been reported by conventional immunofluorescence microscopy that PM cells contain an orthogonal network of actin filaments (AFs) with bundles distributed in parallel and perpendicular to the main ST axis, forming a regular mesh [2, 5].

Peritubular myoid cells contain a myosin smooth muscle isotype, PMC-myosin, whose filaments disassemble in low-strength buffer at 4°C [6].

In preliminary transmission electron microscopy (TEM) studies we observed that the bundles of AF were not distributed in an intermingled mesh, as has been described in PM cells from adult rat testes [2, 5], but were actually arranged in layers.

Endothelin-1 (ET-1) is a peptide synthesized by Sertoli and endothelial cells that acts on PM cells, producing a contraction of the ST. This effect is particularly notable in the ST portion corresponding to stages IX–X of the rat spermatogenic cycle [7, 8]. In this regard, the main objectives of this work were to characterize the organization of both the actin and myosin filaments of PM cells from adult rat testis ST and to determine the changes in the actin cytoskeleton and in the morphological parameters of PM cells during ST contraction with ET-1. To this end, we focused our study on stages IX–X of the ST (subsequently, these will be described as the ST segment) because of their strong ET-1-induced contraction [7, 8]. The ST segments were isolated, and the PM cell morphology and the actin and myosin filament distribution were analyzed by confocal microscopy and TEM in control and ET-1-treated samples.

The knowledge of the cytoskeletal arrangement is vital to the understanding of the role that PM cells play in the contraction of the ST during spermatogenesis.

MATERIALS AND METHODS

The animals used were 3-mo-old Wistar rats born and housed in our animal colony, with a 12L:12D cycle and food and water ad libitum until they were killed by inhalant anesthesia. Animals were maintained in accordance with the National Institutes of Health *Guide for the Care and Use of Laboratory Animals*. In each experiment rats from different breedings were used. All procedures were approved by the Animal Research Committee of the Universidad Nacional de Cuyo. Unless stated otherwise, reagents were purchased from Sigma-Aldrich Chemistry.

Isolation and Treatment of ST Segments

Live-ST segment contraction assays were performed by time-lapse stereomicroscopy to determinate the time necessary to induce the greatest number of ST segments contracted by 50 nM ET-1. We used 50 nM ET-1 in the same way as a recent publication by this laboratory, Fernandez et al. [6], because this concentration induced the same effect as the 100 nM ET-1 used by

[1]Supported by the following grants: 06 J313 and 10 P03 from Secretaría de Ciencia, Tecnología y Posgrado, Universidad Nacional de Cuyo, Argentina; CM 01-03 from Consejo de Investigaciones de la Universidad del Aconcagua, Argentina; and PICT-R 2005-32850 from Agencia Nacional de Promoción Científica y Tecnológica Argentina.
[2]Correspondence: Luis A. Lopez, Laboratory of Cytoskeleton and Cell Cycle, Instituto de Histología y Embriología, Facultad de Ciencias Médicas, Universidad Nacional de Cuyo, Av. Libertador 80, 5500 Mendoza, Argentina. E-mail: llopez@fcm.uncu.edu.ar

Received: 3 August 2011.
First decision: 29 August 2011.
Accepted: 6 February 2012.

eISSN: 1529-7268 http://www.biolreprod.org
ISSN: 0006-3363

Tripiciano et al. [8]. In each experiment, STs from the testes of one rat were dispersed in Dulbecco modified Eagle medium (DMEM)/F12 medium at 37°C in a Petri dish. The ST segments were identified by transillumination [9], dissected with a needle from the rest of the ST, and incubated in DMEM/F12 medium without and with 50 nM ET-1 at 37°C, and time-lapse stereomicroscopy was recorded from Time 0 of incubation. After being recorded, 100 ST segments were separated in contracted and noncontracted groups, fixed with paraformaldehyde, and analyzed by confocal microscopy and TEM in same way as the rest of the samples (see below). This experiment was repeated three times.

To analyze PM cells from control and ET-1-treated ST segments, the following experiment was carried out: STs from the testes of one rat were separated into two groups that were incubated in DMEM/F12 medium without (control) or with 50 nM ET-1 for 3 min at 37°C (ET-1-treated). Both samples were fixed with 4% paraformaldehyde in PBS for 20 min at 37°C or with 5% glutaraldehyde (TAAB) in cacodylate buffer at 37°C for 1 h. After fixation, ST segments were identified by transillumination and dissected with a needle from the rest of the ST. One-micrometer sections of ST segments were stained with toluidine blue and analyzed by light microscopy to confirm that selected segments corresponded to stages IX–X of spermatogenesis. This experiment was repeated three times.

Live-ST Segment Contraction Time-Lapse Stereomicroscopy

Light time-lapse stereomicroscopy was taken of ST segment samples using a Nikon SMZ10 stereomicroscope (Nikon Corp.) with an incubation chamber and a Panasonic Color CCD camera, GP-KR222 (Matsushita Communication Industrial Co. Ltd.). Time-lapse movies of images captured every 2 sec were reviewed and ST segments were scored and analyzed in Image Pro Plus 6.0.0.260 software (Media Cybernetics Inc.). Please see Supplemental *Materials and Methods* (all supplemental data are available online at www.biolreprod.org) for additional information about low-temperature treatment of ST segments and assay of assembled PM cell myosin.

Transmission Electron Microscopy

For each experiment, 50 ST segments from control and ET-1-treated groups were postfixed with 1% osmium tetroxide in cacodylate buffer containing 1% potassium ferrocyanide as an auxiliary membrane contrast agent [10]. Then, ST segments were dehydrated in a graded series of acetone and embedded in low-viscosity resin (Pelco International) as indicated by Spurr [11]. Samples were polymerized in the oven at 70°C for 48 h. Ultrathin sections were obtained in an Ultracut R ultramicrotome (Leica) stained with uranyl acetate and lead citrate [12], and examined in a Zeiss 900 electron microscope.

Immunostaining

For each experiment, 100 ST segments from control and ET-1-treated groups were fixed with 4% paraformaldehyde in PBS for 20 min at 37°C, washed with PBS 3 × 10 min, incubated in 50 mM ammonium chloride in PBS 30 min, rinsed with 0.05% saponin and 0.2% bovine serum albumin in PBS (wash solution) 3 × 10 min, and incubated overnight at 4°C with primary antibodies (Abs). The following Abs were used: monoclonal Ab anti-alpha-actin conjugated with fluorescein isothiocyanate (actin Ab; 1:500; Sigma) or monoclonal Ab anti-smooth muscle myosin type II (myosin Ab; 1:800; Santa Cruz Biotechnology). The samples were rinsed with wash solution (3 × 10 min). The ST segments incubated with myosin Ab were developed with Cy3-conjugated anti-mouse immunoglobulin G Ab (secondary Ab; 1:200; Jackson ImmunoResearch) and then rinsed with wash solution.

For colocalization assays, 50 ST segments from each experiment were incubated with myosin Ab, secondary Ab, myosin Ab again (to block the free Fab regions of the secondary Ab), rinsed with wash solution, and finally incubated with actin Ab or phalloidin-Alexa 488 (1:250; Invitrogen). To check the specificity of the secondary Ab, this assay was repeated without myosin Ab.

The immunostaining preparations were embedded in NP-gallate mounting medium, coverslipped, and examined with a confocal microscope (FV 1000; Olympus) with a Paplon 60× lens.

Appropriate controls were included to ensure that the staining observed was specific. (See *Results* and Supplemental Figs. S2–S4.)

Image Capture and Processing

Serial confocal optical sections (OSs) were taken throughout the depth of the ST segment with a step size of 200 nm. The first OS was taken at the deepest level of the PM cell (near the epithelium) when the first filament image was detected. Consecutive OSs were taken until the last filament image was detected at the most superficial level of the PM cell (near the interstitium).

Morphological Parameters

The diameters of 50 ST segments from each live-ST segment contraction time-lapse stereomicroscopy assay were measured in pictures taken in a Nikon SMZ10 stereomicroscope using Image J software [13].

The diameters of ST segments, the cellular area, the x and y diameters (parallel and perpendicular to the main ST axis, respectively), and the AF layer thickness of 10 PM cells from each ST segment were calculated in tangential confocal images of 50 ST segments stained with actin Ab using Image J software. The AF layer thickness of AFs perpendicular or longitudinal to the main ST axis was calculated by the sum of serial OSs taken from the deepest to the most superficial levels of PM cells.

Quantitative Colocalization Analysis

The colocalization analysis was made using the JACoP plugin for Image J software according to Bolte and Cordelieres [14]. Z-Stack images of 100 PM cells from 20 ST segments stained for both actin and myosin were deconvolved. The channel-specific point spread functions were generated and the signal:noise ratio was adjusted until deconvolved images were free of pixel noise and the colocalization analysis was made using two correlation coefficients, Pearson (PCC) and Manders (MCC).

For PCC calculation, the dependency of pixels in dual-channel images (green and red channels for AFs and myosin filaments [MyFs], respectively) was measured by plotting the pixel gray values of two images against each other. These values were displayed in a pixel-distribution diagram (scatter plot), and a linear equation of the relation between the intensities of the two images was calculated by linear regression. A cross-correlation function (CCF) was obtained by plotting the corresponding PCC for each pixel shift (delta x) of the green image in the x direction relative to the red image. The real value of the PCC is estimated at delta $x = 0$. This value can range from 1 to −1, with 1 standing for complete positive correlation, −1 for negative correlation, and 0 for no correlation.

The MCC is based on the PCC, with average intensity values being taken out of a mathematical expression [15]. Two coefficients were obtained, MCC-M1 and MCC-M2, for the fraction of AFs overlapping with MyFs and for the fraction of MyFs overlapping with AFs, respectively. These values vary from 0 to 1, corresponding to nonoverlapping images or complete colocalization, respectively.

Statistical Procedures

The data from each assay are expressed as the average of three experiments ± SEM. Statistical significance was assessed with Student t-test. $P \leq 0.05$ was considered significant.

RESULTS

Confocal Image of AFs

By confocal microscopy, we could observe bundles of AFs in a particular arrangement in PM cells of the ST segment. In the deepest inner OSs, toward the seminiferous epithelium, the AFs were oriented perpendicularly to the main ST axis (Fig. 1a). This set of AFs will be described henceforth as the inner circular layer. After several sections, in the medial OSs, new bundles of AFs with orientation parallel to the main ST axis appeared together with the inner circular layer (Fig. 1a′). Toward the interstitium, in the external OSs, only bundles of AFs with parallel orientation remained (Fig. 1a″). This set of parallel AFs will be described henceforth as the external longitudinal layer. The Z-Stack of successive OSs is shown in Figure 1a‴. In addition to longitudinal and circular AF bundles, there were peripheral AF bundles forming a cortical belt around the cell (Fig. 1a‴).

In each PM cell, many of the AF bundles corresponded with those with the same orientation in the neighboring PM cells (Fig. 1a‴).

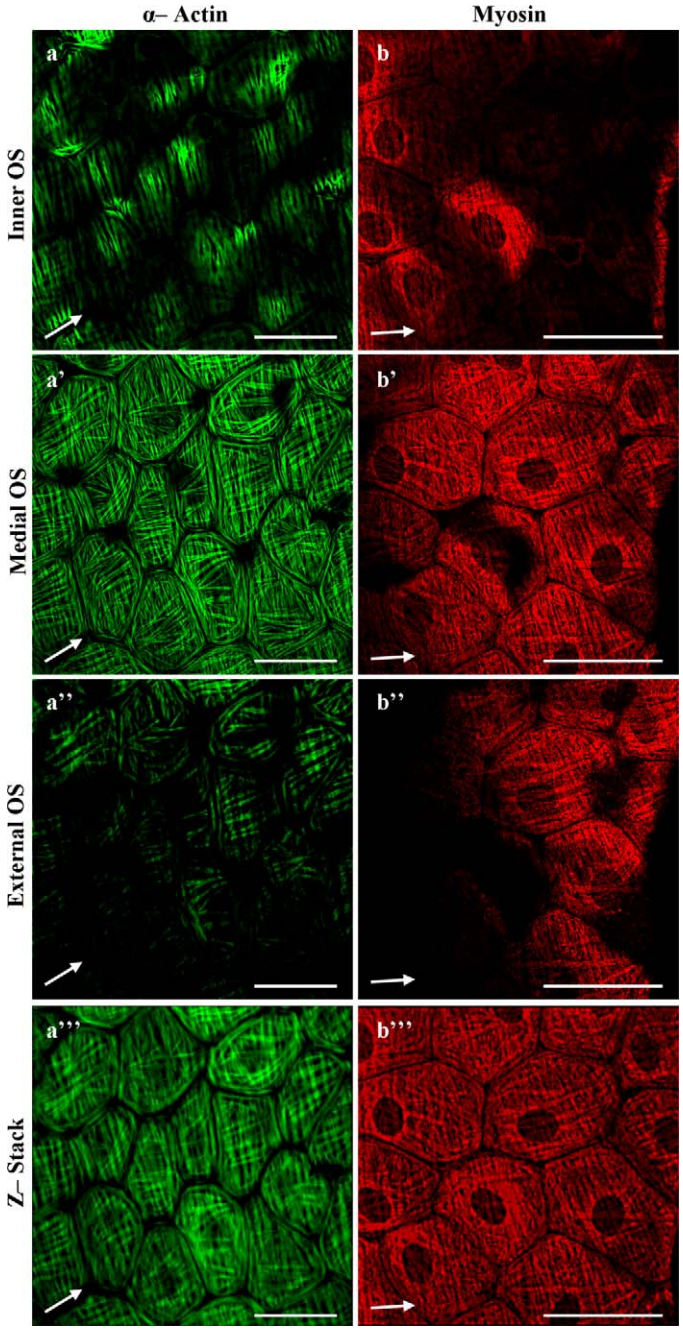

FIG. 1. Peritubular myoid cells observed by confocal microscopy. **a**–**a‴**) Staining with actin Ab. **b**–**b‴**) Staining with myosin Ab. **a** and **b**) Inner OS. **a′** and **b′**) Medial OS. **a″** and **b″**) External OS. **a‴** and **b‴**) Compressed Z-Stack of successive OSs. Main longitudinal axis of the ST (arrow). Bars = 50 μm. An animation of the successive OSs of AF from the deepest to the most superficial level of the PM cells is shown in Supplemental Video 1.

An animation of the successive OSs of AFs from the deepest to the most superficial level of the PM cells described above is shown in Supplemental Video 1.

TEM Analyses of AFs

Using TEM, we observed that AFs were distributed in two layers in PM cells (Fig. 2a). In the inner cytoplasmic zone, between the nucleus and the plasma membrane toward the seminiferous epithelium, AFs were oriented perpendicularly to the longitudinal ST axis and corresponded to the inner circular layer described above. In the external cytoplasmic zone, between the nucleus and the plasma membrane toward the interstitium, AFs were oriented parallel to the ST axis and represented the external longitudinal layer described above (Fig. 2a′). It is worth mentioning that the inner circular layer was observed in any field of the PM cell sections, whereas the external longitudinal layer was more often seen above the nuclear zone (data not shown).

Because of these observations, we conclude that AF bundles in PM cells actually exist in two independent layers: the inner circular and the external longitudinal ones.

Confocal Image of MyF

Immunostaining with the myosin Ab showed the presence of MyFs in PM cells (Fig. 1, b–b‴). The secondary Ab used reacted specifically with the myosin Ab (see below, *Colocalization of AF and MyF*).

An inner circular layer of MyF was observed in the inner OS of PM cells (Fig. 1b). Subsequently, medial OSs presented MyF bundles with both perpendicular and parallel orientations with respect to the main ST axis (Fig. 1b′). And finally, in the most superficial OSs, an external longitudinal layer of MyF was present (Fig. 1b″). The Z-Stack of successive OSs is shown in Figure 1b‴.

A strong myosin stain surrounding the nucleus was observed, possibly corresponding to the anchorage of MyF to the nuclear envelope (Fig. 1b‴), but MyFs were not found in the cell peripheral belt where AF bundles were present (compare Fig. 1, a‴ with b‴).

Colocalization of AF and MyF

To perform colocalization assays of AF-MyF in PM cells, ST segments were stained with both actin and myosin Abs.

To confirm that each corresponding primary Ab reacts specifically with AF or MyF, we carried out two controls. First, we disassembled the MyF at 4°C before staining (the depolimerization was confirmed by Western blot analysis; Supplemental Fig. S1).

The immunostaining showed that AFs after 4°C treatment maintained the same pattern as AFs after 37°C treatment. On the contrary, MyF staining disappeared almost completely after 4°C treatment, indicating that the anti-myosin Ab used does not cross-react with AF, and that the actin Ab does not react with the secondary Ab present (Supplemental Fig. S2). The second control consisted in the use of phalloidin-Alexa 488 to decorate AFs in place of actin Ab, whereas MyFs were labeled as before. Again, in this control, AF and MyF showed the same pattern that was observed above using both primary Abs (Supplemental Fig. S3). Hereafter, in the following experiments in this study, we will use the actin Ab to recognize AF because phalloidin reacts with both alpha- and beta-actin. Consequently, the staining of AF with phalloidin does not distinguish AFs in PM cells from those in other ST cells.

On the other hand, to discard a nonspecific reaction of the secondary Ab used to visualize myosin, we repeated the staining using the myosin secondary Ab and the actin primary Ab. As can be seen in Supplemental Figure S4, this combination gave no staining.

The simultaneous staining of AF and MyF in the PM cells of ST segments shows that AF colocalized with MyF (Fig. 3). To determine the degree of AF-MyF colocalization, we used PCC, MCC-M1, and MCC-M2.

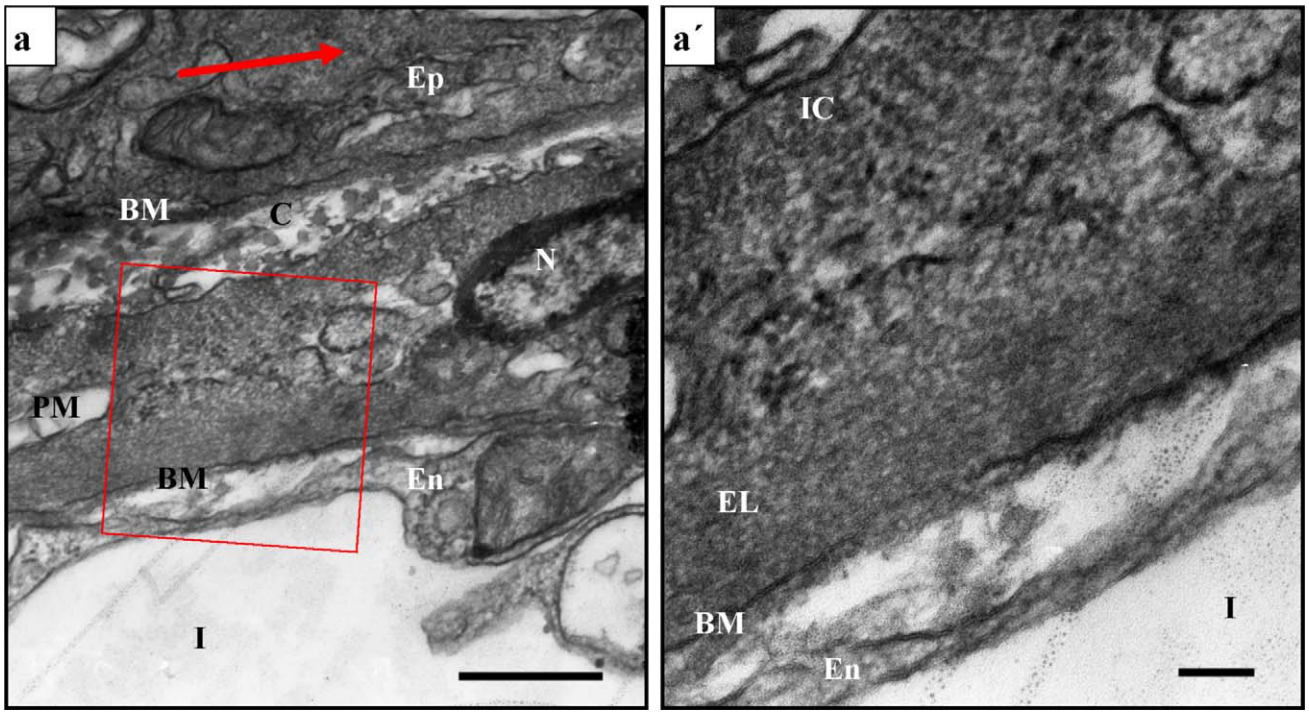

FIG. 2. Electron microscopy of longitudinal section of an ST segment. **a**) The PM cell lies between seminiferous epithelium (Ep) and the endothelium (En) close to the interstitium (I). N, PM cell nucleus; BM, basement membrane; C, collagen fibers. The boxed area is shown at a higher magnification in **a**′. **a**′) Inner circular layer (IC) and external longitudinal layer (EL) of AFs oriented perpendicularly and in parallel, respectively, to the main axis of the ST. Main longitudinal axis of the ST (arrow). Bars = 0.5 μm (**a**) and 0.1 μm (**a**′).

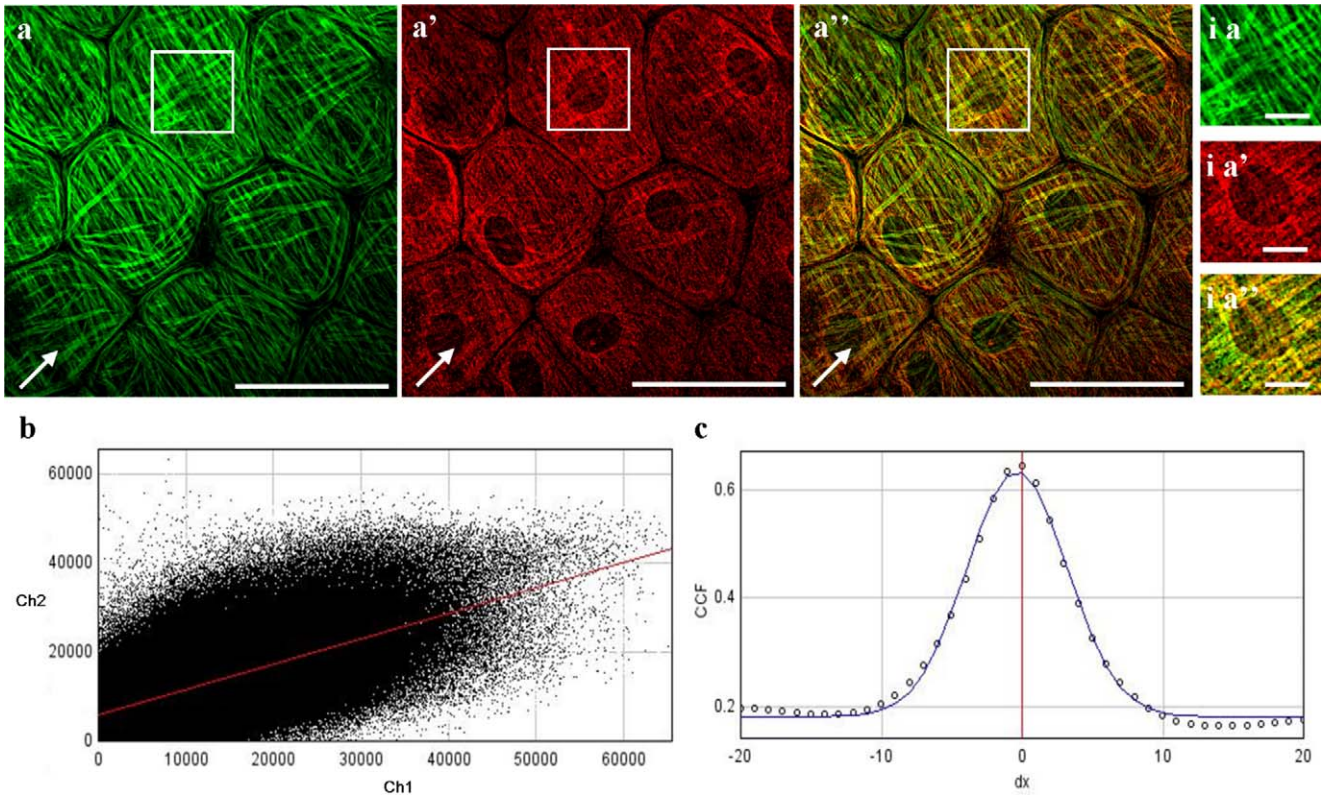

FIG. 3. Colocalization of AF and MyF in PM cells. **a**–**a**″) Peritubular myoid cells observed by confocal microscopy. **a**) AF. **a**′) MyF. **a**″) Merged. **i a**, **i a**′, and **i a**″) Insets at higher magnifications of boxed areas in **a**, **a**′, and **a**″, respectively. **b** and **c**) Colocalization analysis with JACoP. **b**) Scatter plot of colocalization event for MyF (Ch2) versus AF (Ch1). **c**) Cross-correlation function: PCCs versus pixel shift (dx). Main longitudinal axis of the ST (arrow). Bars = 50 μm (**a**–**a**″) and 10 μm (**i a**–**i a**″).

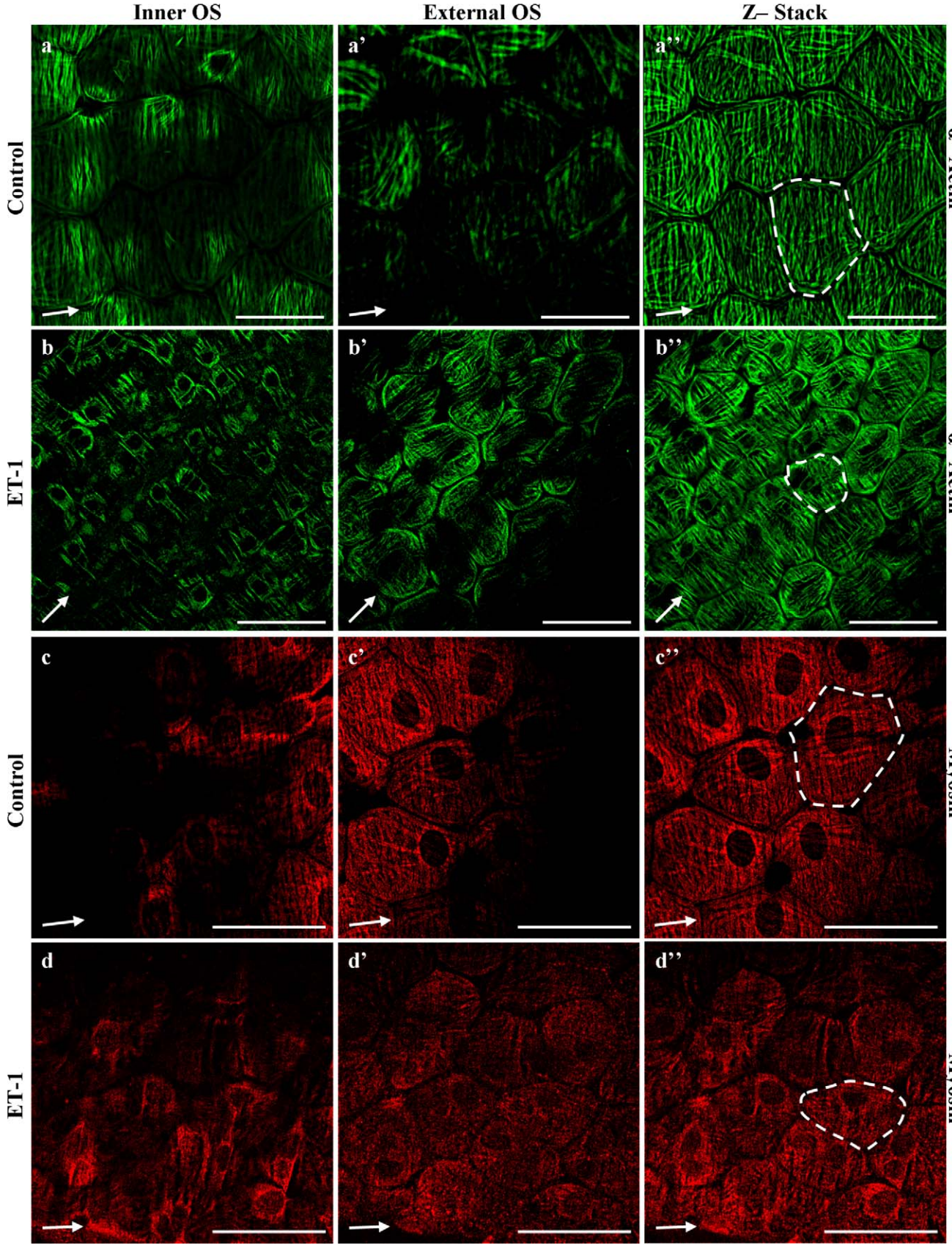

FIG. 4. The PM cells from control and ET-1 contracted ST segments observed by confocal microscopy. **a**–**a**″ and **c**–**c**″) Control ST segments. **b**–**b**″ and **d**–**d**″) ET-1 contracted ST segments. **a**, **b**, **c**, and **d**) Inner OS. **a**′, **b**′,**c**′, and **d**′) External OS. **a**″, **b**″, **c**″, and **d**″) Z-Stack of every OS. **a**–**b**″) Staining with actin Ab. **c**–**d**″) Staining with myosin and secondary Abs. The dashed lines delimit the extent of the PM cell. Main longitudinal axis of the ST (arrow). Bars = 50 μm.

TABLE 1. Morphological parameters of PM cells.

Parameter	Control	ET-1[a]	Change (%)
Tangential area (μm^2)	1823.1 ± 68.8	1127.0 ± 77.9**	−38.3 ± 2.16
x Diameter (μm)	43.9 ± 1.7	39.2 ± 1.9*	−10.7 ± 2.54
y Diameter (μm)	48.4 ± 1.7	35.2 ± 1.5**	−27.3 ± 3.52
Height (μm)	3.33 ± 0.17	4.78 ± 0.4	+43.7 ± 11.06

[a] ET-1 (ET-1 contracted ST segments).
* $P \leq 0.03$, ** $P \leq 0.008$ compared with control.

TABLE 2. Height of AF layers of PM cells from control and ET-1 contracted ST segments (ET-1).

AF layer thickness (μm)	Control	ET-1	Change (%)
Inner circular	1.38 ± 0.09	2.57 ± 0.4**	+90.22 ± 28.92
External longitudinal	0.45 ± 0.03	0.78 ± 0.09*	+79.94 ± 17.51

* $P \leq 0.03$, ** $P \leq 0.009$ compared with control.

The value of PCC was 0.646, indicating that the scatter plot distribution corresponds to partial colocalization (Fig. 3b). In addition, the shape of the CCF curve indicated a nonrandom partial colocalization (Fig. 3c). However, using a coefficient independent of stain intensity, MCC [14], we found that MCC-M1 was 0.949 and MCC-M2 was 0.947. These values near to 1.0 indicate that the colocalization of AF and MyF was almost complete. These results implicate that the AF and MyF in the PM cell are arranged in myofibers, as in smooth muscle cells.

Cytoskeleton of PM Cells from ET-1-Treated STs

We used 50 nM ET-1 to contract ST segments, according to Fernandez et al. [6]. This concentration induced the same effect as that of the 100 nM ET-1 used by Tripiciano et al. [8] (data not shown). By light time-lapse stereomicroscopy, we observed that the maximal number of contracted ST segments of the sample (60.1% ± 3.8%) was reached during the first 3 min of ET-1 treatment. The characteristics of contracted ST segments were: winding movements, diameter reduction, and expulsion of the ST segments contents from their extremes (data not shown). This population of contracted ST segments will be described henceforth as ET-1 contracted ST segments. The remaining 40% of the ST segments of the sample did not show any of the characteristics of contracted ST segments described above, and will be described henceforth as ET-1 noncontracted ST segments.

After 3 min of treatment without ET-1 (control), ST segments had a diameter of 315.8 ± 8.4 μm. Meanwhile, after 3 min of treatment with 50 nM ET-1, the population of contracted ST segments had a diameter of 237.9 ± 9.1 μm, which represents a statistically significant reduction of 24.6% ($P \leq 0.002$) compared with the diameter of control ST segments. The population of noncontracted ST segments had a diameter of 327.3 ± 12.9 μm, which is not significantly different from the diameter of control ST segments.

To analyze the effect of ET-1 on ST segments by confocal microscopy, only ET-1-treated ST segments with a 230- to 250-μm diameter (ET-1 contracted ST segments) were analyzed. ET-1-treated ST segments with a 300- to 350-μm diameter were considered noncontracted and discarded.

By confocal microscopy we observed that PM cells from ET-1 contracted ST segments became more rounded than the control ST segments (Fig. 4, b″ and d″). The tangential area of PM cells was reduced 38% (Table 1), and the *x* and *y* diameters of individual PM cells were shortened by 10.7% and 27.3%, respectively (Fig. 4 and Table 1). In addition, the height of PM cells increased by 41.4% (Table 1).

The AFs of PM cells from ET-1 contracted ST segments maintained their arrangement in two independent layers (Fig. 4, b and b′). However, the AF bundles of the external longitudinal layer became organized in compact ribbons (Fig. 4b′). Furthermore, the height of the inner circular and external longitudinal layers of AFs increased by 90.2% and 79.9%, respectively (Table 2).

The immunostaining of myosin in PM cells from ET-1 contracted ST segments showed that MyFs were distributed in two independent layers, as in PM cells from control ST segments (Fig. 4, d–d″), although the MyF bundles of the external longitudinal layer became organized in compact ribbons (Fig. 4d′).

When observed with TEM, ET-1 contracted ST segments presented contracted PM cells with deep folds in the nuclear envelope (Fig. 5b). The height of the PM cells at the nuclear region was greater in treated than in control STs (Fig. 5, b and d), and both the epithelial and the endothelial BMs appeared more waved (Fig. 5, b and d).

In addition, contracted PM cells maintained the arrangement of the AF in two layers (Fig. 5, b and d), even though the AF bundles were more interwoven and anchored to the plasma membrane than in the control (Fig. 5, d and d′).

DISCUSSION

In this communication we describe the organization of AF-MyF of PM cells from control and ET-1 contracted ST segments. The results obtained by confocal microscopy were complemented with TEM.

AFs and MyFs in PM Cells

We found that PM cells have AF-MyFs distributed in thick bundles, AF-MyF bundles, in two independent layers: the inner circular toward the seminiferous epithelium and the external longitudinal toward the interstitium. In both layers, AFs and MyFs colocalize almost completely.

Using confocal microscopy, we observed an intermediate zone with AF-MyF bundles oriented in two directions between the inner circular and external longitudinal layers, which could be interpreted as a third layer with the two types of filaments in an orthogonal arrangement. However, the PM cell slices taken through the filament layers and observed by TEM did not show the presence of a third layer and confirm that there are really only two layers of filaments. Thus, the intermediate zone of AF-MyF bundles observed by confocal microscopy may indicate leakage of the filaments' fluorescence between the inner and the external layers.

As far we know, this is the first time that two independent layers of AF-MyFs with different orientations have been described in PM cells. Previous studies in these cells, also using confocal microscopy, described AFs as being distributed in a unique layer, forming a regular orthogonal mesh [2, 5]. Moreover, using TEM, Maekawa et al. [5] described AFs running in cross and longitudinal sections in the inner cytoplasmic zone. Our results differ from those of previous investigators [2, 5], probably because we could take advantage of the analysis of the Z-Stack images by confocal microscopy, and we have taken great care in the positioning of the filaments with respect to the main ST axis in all of the samples analyzed by TEM.

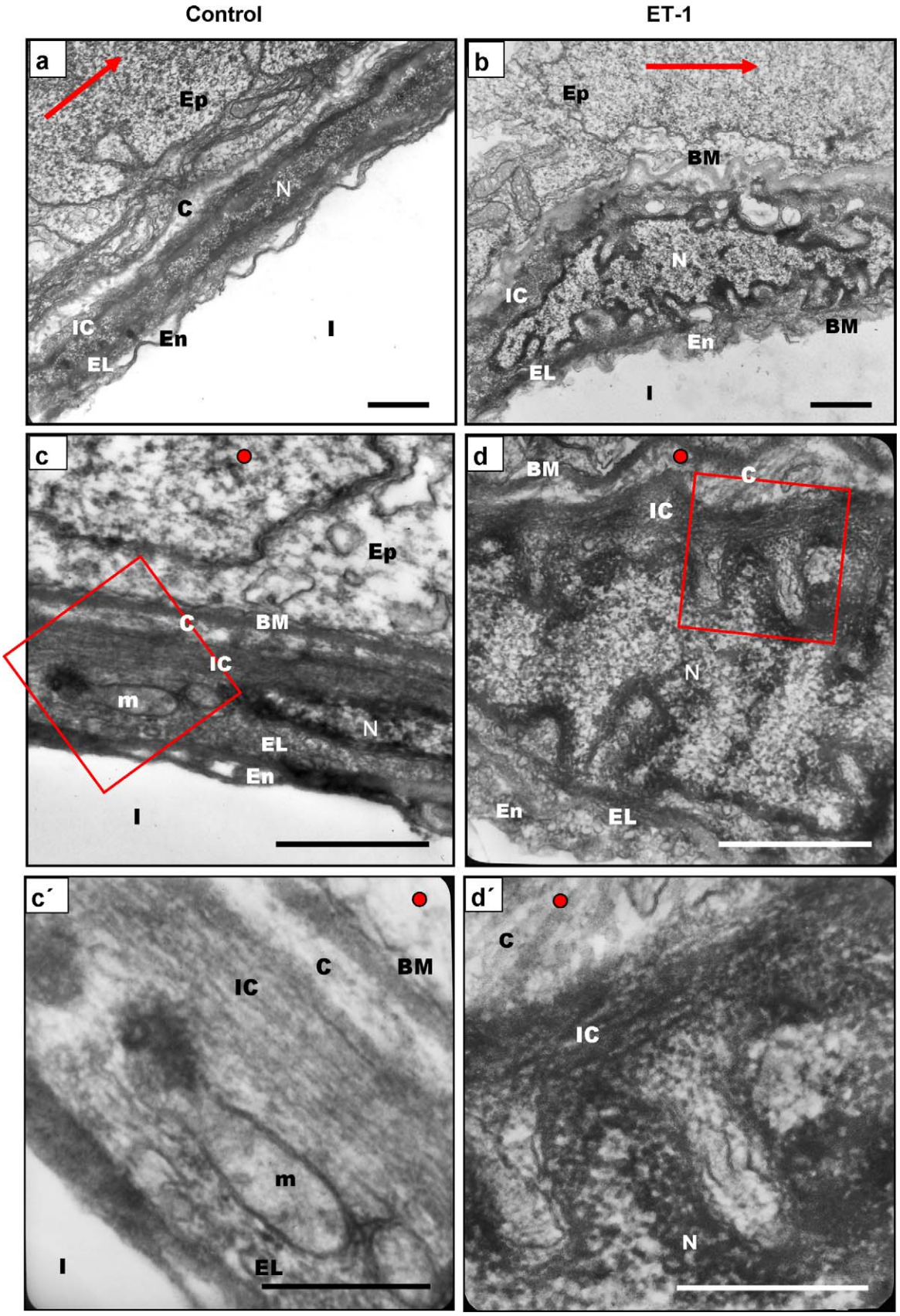

FIG. 5. Electron microscopy of control and ET-1 contracted ST segments. **a**) Longitudinal section of control ST segment. The PM cell looks flat and relaxed, with an elongated nucleus (N). **b**) Longitudinal section of ET-1-treated ST. **c**) Cross section of a control ST segment showing a relaxed PM cell. Boxed area is shown at a higher magnification below in **c**′. **c**′) The AF of the inner circular layer (IC). **d**) Cross section of ET-1 contracted ST showing a contracted PM cell. Boxed area is shown at a higher magnification below in **d**′. **d**′) The AF of the inner circular layer (IC). BM, basal membrane; C, collagen fibers; En, endothelium; EL, external longitudinal layer; I, interstitium; m, mitochondria; Ep, seminiferous epithelium. In **a** and **b**, the main longitudinal axis of the ST is indicated by a red arrow. In the remaining panels the longitudinal axis is indicated by a cross section of the arrow that appears as a red spot. Bars = 1 μm (**a**–**d**), 0.1 μm (**c**′ and **d**′).

AFs and MyFs in PM Cells of Contracted STs

When ST segments were contracted with ET-1, PM cells increased their height, reduced their tangential area, and also decreased both *x* and *y* diameters. These results indicate that PM cells changed shape, becoming taller and rounded. It seems that PM cells are able to produce contractile force in two directions, even thought the contraction perpendicular to the main ST axis is more pronounced.

We found that AF-MyF bundles in contracted ST segments maintained the same organization in two layers, although they appear thicker and more interwoven. Also, the AF-MyFs of the external longitudinal layer became organized in compact ribbons above the cell nucleus.

Tripiciano et al. [8] described the effect of ET-1 as turning the actin orthogonal meshwork of PM cells into a ring around the nucleus; however, according to our results, the AFs conserve their organization in two layers.

PM cells express the same contractile proteins as smooth muscle cells and share several structural aspects, such as numerous caveoli and the presence of BM surrounding the cell [16]. However, there are some differences with smooth muscle cells. For example, in the small intestine, the smooth muscle cells present a fusiform shape and contain AF-MyFs running longitudinally to the main cellular axis. For this reason smooth muscle cells only contract along one axis. Meanwhile, PM cells present a flat polygonal shape and contain AF-MyFs assembled in two layers orientated perpendicularly to each other. Consequently, they are able to contract in two directions, as we showed in this work.

Interestingly, Tripiciano et al. [8] found that PM cells coexpress ET_A and ET_B receptors that act through different intracellular signaling pathways. They proposed an analogy between the contraction of ST with intestinal peristalsis [8]. The intestinal smooth muscle cells are arranged in two differently oriented sheets: longitudinal and circular with respect to the main gut axis. The contraction of intestinal longitudinal muscle is activated through a different intracellular signaling pathway than the circular muscle. Conversely, the PM cells are arranged in a single layer in the rat. The ET_A and ET_B receptors respond to ET-1 stimulation in virtually every single PM cell [8], raising the possibility that in each cell the two directions of contraction could be operated through either ET_A or ET_B stimulation acting through different mechanisms. The flux of tubular fluid and spermatozoa might result from the combined circular and longitudinal contraction of the PM cell monolayer. In this way, the fact that AF-MyFs are organized in two independent layers that contract in orthogonal directions, as we have shown in this work, reinforces the hypothesis of Tripiciano et al. [8], because each ET-1 receptor could mediate the contraction of one of the layers.

Further studies in this model should be carried out to understand whether one stimulus can produce a preferential contraction of a single AF-MyF layer in the PM cells.

The behavior of the contractile machinery in the ST segments during the other stages of the spermatogenic cycle remains to be studied. For example, in stages VII–VIII (prior to spermiation) PM cell tone may be stronger because of the need to expel spermatozoa into the ST lumen against a greater resistance exerted by a taller epithelium.

In our communication, the data obtained in sequential longitudinal sections from PM cells by confocal microscopy were complemented with data obtained from cross sections by TEM. We consider that this approach is a good example of how two different techniques—confocal and electron microscopy—can complement each other to reach a more accurate interpretation of cellular morphology.

ACKNOWLEDGMENT

We thank M. Aguilera for technical assistance with the colocalization assays and S. Patterson for correction of the English.

REFERENCES

1. Palombi F, Salanova M, Tarone G, Farini D, Stefanini M. Distribution of beta 1 integrin subunit in rat seminiferous epithelium. Biol Reprod 1992; 47:1173–1182.
2. Vogl AW, Soucy LJ, Lew GJ. Distribution of actin in isolated seminiferous epithelia and denuded tubule walls of the rat. Anat Rec 1985; 213:63–71.
3. Hadley MA, Dym M. Immunocytochemistry of extracellular matrix in the lamina propria of the rat testis: electron microscopic localization. Biol Reprod 1987; 37:1283–1289.
4. Tung PS, Fritz IB. Characterization of rat testicular peritubular myoid cells in culture: alpha-smooth muscle isoactin is a specific differentiation marker. Biol Reprod 1990; 42:351–365.
5. Maekawa M, Kamimura K, Nagano T. Peritubular myoid cells in the testis: their structure and function. Arch Histol Cytol 1996; 59:1–13.
6. Fernandez D, Bertoldi MV, Gomez L, Morales A, Callegari E, Lopez LA. Identification and characterization of Myosin from rat testicular peritubular myoid cells. Biol Reprod 2008; 79:1210–1218.
7. Tripiciano A, Filippini A, Giustiniani Q, Palombi F. Direct visualization of rat peritubular myoid cell contraction in response to endothelin. Biol Reprod 1996; 55:25–31.
8. Tripiciano A, Palombi F, Ziparo E, Filippini A. Dual control of seminiferous tubule contractility mediated by ETA and ETB endothelin receptor subtypes. FASEB J 1997; 11:276–286.
9. Parvinen M, Vanha-Perttula T. Identification and enzyme quantitation of the stages of the seminiferous epithelial wave in the rat. Anat Rec 1972; 174:435–449.
10. Karnovsky MJ. Use of ferrocyanide-reduced osmium in electron microscopy. J Cell Biol 1971; 51:146–147.
11. Spurr AR. A low-viscosity epoxy resin embedding medium for electron microscopy. J Ultrastruct Res 1969; 26:31–43.
12. Reynolds ES. Use of lead citrate at hight pH as an electronopaque stain in electron microscopy. J Cell Biol 1963; 17:208–213.
13. Rasband WS. Image J. Bethesda, MD: National Institutes of Health; 1997–2006. http://rsb.info.nih.gov/ij/. Accessed October 28, 2003.
14. Bolte S, Cordelieres FP. A guided tour into subcellular colocalization analysis in light microscopy. J Microsc 2006; 224:213–232.
15. Manders EM, Stap J, Brakenhoff GJ, van Driel R, Aten JA. Dynamics of three-dimensional replication patterns during the S-phase, analysed by double labelling of DNA and confocal microscopy. J Cell Sci 1992; 103: 857–862.
16. Virtanen I, Kallajoki M, Narvanen O, Paranko J, Thornell LE, Miettinen M, Lehto VP. Peritubular myoid cells of human and rat testis are smooth muscle cells that contain desmin-type intermediate filaments. Anat Rec 1986; 215:10–20.